# Topological defects, orientational order, and depinning of the electron solid in a random potential

Min-Chul Cha and H.A. Fertig
*Center for Computational Sciences and Department of Physics and Astronomy, University of Kentucky, Lexington, Kentucky 40506-0055*
(Received 15 July 1994)

We report on the results of molecular-dynamics simulation studies of the classical two-dimensional electron crystal in the presence of disorder. Our study is motivated by recent experiments on this system in modulation-doped semiconductor systems in very strong magnetic fields, where the magnetic length is much smaller than the average interelectron spacing $a_0$, as well as by recent studies of electrons on the surface of helium. We investigate the low-temperature state of this system using a simulated-annealing method. We find that the low-temperature state of the system always has isolated dislocations, even at the weakest disorder levels investigated. We also find evidence for a transition from a hexatic glass to an isotropic glass as the disorder is increased. The former is characterized by quasi-long-range orientational order, and the absence of disclination defects in the low-temperature state, and the latter by short-range orientational order and the presence of these defects. The threshold electric field is also studied as a function of the disorder strength, and is shown to have a characteristic signature of the transition. Finally, the qualitative behavior of the electron flow in the depinned state is shown to change continuously from an elastic flow to a channel-like, plastic flow as the disorder strength is increased.

## I. INTRODUCTION

Sixty years ago, Wigner[1] predicted that at low enough densities, the ground state of a collection of electrons should have a crystalline form. Convincing evidence of this Wigner crystal (WC) was first reported by Grimes and Adams[2] 45 years later for a collection of electrons on the surface of He. This system is at such low densities that exchange effects among the electrons are negligible, so that for all intents and purposes, it may be regarded as purely classical.

More recently, there have been a number of studies searching for the WC in semiconductor systems, where considerably higher densities may be obtained. A major drawback of semiconductors is that one usually needs to introduce (randomly located) dopants in order to put free electrons into the system. These dopants then become a source of disorder, which competes with the intrinsic tendency of low-density electrons to form an ordered solid in their ground state. Indeed, in a bulk doped semiconductor, electrons usually bind to the charged donors at zero temperature, forming a completely *disordered* state in this limit.

Great progress has been made on semiconductor systems since the invention of modulation doping.[3] In this class of materials, a two-dimensional layer of electrons ("two-dimensional electron gas," or 2DEG) is collected at the interface of two different semiconductors (typically, GaAs and $Al_xGa_{1-x}As$), with the donor atoms set back by some distance $d$ from the electron layer. By fabricating a sample with a large ratio $d/a_0$, where $a_0$ is the lattice constant of a perfect electron lattice, the greatest source of randomness is relatively far from the electrons, and disorder effects become much less pronounced. (Indeed, in situations where they do not crystallize, the electrons have remarkably high mobilities, suggesting that the electrons undergo very little elastic scattering.[4,5]) This sytem has thus become one of the leading candidates for the observation of a WC.

This paper studies, using computer simulations, the low-temperature properties of the two-dimensional WC, in the low-density limit, where the electrons may be treated as classical. Many of our results will also be applicable for higher-density electron systems in the presence of very strong magnetic fields. Our primary focus will be on low-temperature configurations and how they are affected by disorder, and on the behavior of the electrons in the presence of an electric field (i.e., depinning properties).

The application of a strong, perpendicular magnetic field further enhances the prospects of stabilizing a WC in the 2DEG. In the absence of a magnetic field, the zero-point kinetic energy cost of localizing electrons at lattice sites competes with the potential energy gained by forming a lattice; at high enough densities, the former will always destabilize the lattice. By contrast, in a magnetic field $B$ electrons may be localized to within a length scale $l_0 = \left(\frac{\hbar c}{eB}\right)^{1/2}$, and simultaneously have their lowest possible kinetic energy. Since $l_0$ becomes arbitrarily small in the high field limit, one may form highly localized wave packets, from which a WC state may be constructed. Furthermore, for $l_0 \ll a_0$, exchange effects are negligible,[6] and the ground state of the system may in a sense be regarded as the *classical* ground state of the electron system: the electron wave packets form a crystalline state, and the potential energy of the configu-

 

ration is given to an excellent approximation by the classical configuration energy.[7] Because most of the results presented here — specifically, low-temperature configurations and depinning fields — are essentially static properties of the electrons, they should be applicable in the presence of strong enough magnetic fields that exchange effects may be ignored.

Many investigations of systems in the limit $l_0 \ll a_0$ for the GaAs system showed some signs of behavior associated with the WC.[8] In particular, samples with setback ratios $d/a_0$ of the order 3–4 and larger have been found to be strongly insulating in the limit of low temperature.[9] This behavior is consistent with a crystalline ground state, which is pinned by an arbitrarily weak impurity potential,[10] and hence will not carry current in weak electric fields. Experiments on samples with still higher setback ratios $d/a_0$, and remarkably high mobilities, have shown other signatures of WC behavior.[4,5] A depinning[10,11] threshold as a function of applied voltage has been observed,[4,12,13] and broadband noise in the current is seen to emerge above the depinning transition.[14] (However, narrow-band noise — often seen in charge density wave systems[11] — has not been observed.[14]) Our simulations address this phenomenology, and in particular attempt to sort out both the qualitative and quantitative changes in depinning behavior as the strength of the disorder is varied.

As pointed out above, in the low-density limit, the 2DEG may be treated as classical. Using a combination of molecular-dynamics (MD) methods and analysis using continuum elasticity theory, we have studied the effect that a disorder potential has on the classical WC. In this work, we report the results and details of our numerical simulations. Our continuum elasticity theory analysis will be presented in detail elsewhere,[15] although some of the results of that work will be explained below. Some of the results discussed here have been reported previously.[16] The questions we wish to address are as follows: (1) Is there a qualitative difference among the ground states of samples subject to different levels of disorder, or are they the same, with different correlation lengths? (2) How does the depinning threshold electric field vary with the strength of disorder? (3) How does the current flow when the crystal is depinned, and in what situations might one expect to observe narrow-band and/or broadband noise?

To be specific, we focus on modulation-doped semiconductors as our model system, and control the strength of disorder by varying the ratio $d/a_0$. Experimentally, this may be controlled either by fabricating several samples with different values of $d$, or by varying the density of electrons in a single sample (for example, via a gate geometry). Our study is also directly applicable to studies of electrons on thin helium films, where disorder may be introduced by using a glass slide substrate[17] as well as to charged polystyrene sphere systems suspended in water.[18] We focus on the extent of order in typical low-temperature states, which are generated using a simulated-annealing method. We will present evidence that there is a zero-temperature phase transition in this system as a function of $d/a_0$, from a state with power-law behavior in the orientational correlation function to one with an exponential falloff, as $d$ is decreased. We call the former state a hexatic glass, and the latter an isotropic glass. This transition suggests that there is not just a quantitative, but rather *qualitative* difference among the zero-temperature states of electron layers subject to different levels of disorder.

We also study how current flows at low temperature for the different types of ground states, using our MD simulations, in the presence of an electric field. We compute the depinning field $E_{th}$ as a function of $d/a_0$, and there find direct evidence of the phase transition. To our knowledge, this is the first suggestion that depinning properties of a solid may be used to probe a structural phase transition. We will demonstrate a striking difference in the current flow patterns of the two cases. For the hexatic glass, we find an essentially elastic flow of the electrons just above the depinning transition; i.e., all the electrons participate in the conduction, and maintain roughly a constant position with respect to the moving center of mass. In the isotropic glass, we find a more plastic flow, in which the crystal "tears"; in the most strongly disordered cases, large patches of electrons may be completely immobilized, while the rest of the electrons carry the current. Some consequences of the motion for the noise spectrum will also be discussed.

This paper is organized as follows. For readers interested just in our results, Sec. II describes our model, and then discusses our principal findings. Readers interested in the details of our calculations may find our molecular-dynamics and simulated-annealing methods described in Sec. III. Section IV describes the calculations of depinning fields and current patterns, and we conclude with a summary in Sec. V.

## II. MODEL AND RESULTS

Our model system for the disordered WC is motivated directly by the modulation-doped systems described in the Introduction. We consider two planes of charges (Fig. 1). One contains $N$ electrons that are free to move within the plane in response to any forces exerted upon them. The other contains $N$ positively charged ions which are quenched; i.e., fixed in position. These ions are placed in the plane completely randomly, with no corre-

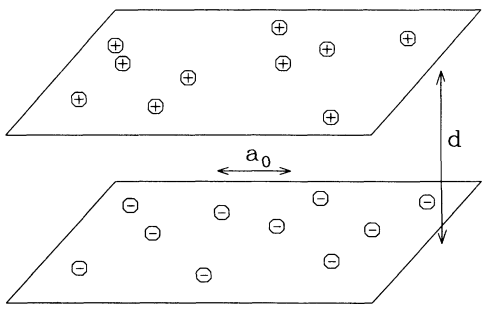


FIG. 1. Model system of $N$ electrons and $N$ quenched positively charged ions, in planes separated by a distance $d$.

lation among the ion positions. The ion layer is set back from the electron layer by a distance $d$, which controls the strength of the disorder. The electrons and ions interact via the usual Coulomb potential, with a dielectric screening constant $\kappa = 13$, as would be appropriate for a GaAs system. We focus on the low-temperature states of the electrons using a simulated-annealing method, which will be described in detail in Sec. III. We have studied system sizes up to $N$=3200 electrons (and 3200 ions), and employ periodic boundary conditions. Our electron density in these simulations is taken to be $5.7 \times 10^{10}$ cm$^{-2}$. We study both the low-temperature configurations of the electrons, and their response (i.e., motion) when an electric field is turned on. The latter is studied using direct molecular-dynamics simulations of the classical motion of the electrons; this is described in detail in Sec. IV.

The ground states that we find, for *arbitrarily large* values of $d$, are never crystalline: the positional correlation function falls off *exponentially*; i.e., there is short-range positional order. Such states are most properly classified as glasses. It is well known that any coupling of randomness to an otherwise perfect crystal will destroy the long-range positional order[19] normally associated with a crystal in two dimensions. However, at a minimum this occurs because of smooth fluctuations that are forced into the crystal to optimize the total energy (including coupling to the disorder). These may be described by a displacement field $\vec{u}(\vec{R})$, where $\{\vec{R}\}$ are the lattice sites of the perfect crystal, which varies slowly on the length scale $a_0$. Such a state has a *power-law* decay in the positional correlation function,[20,21] which is sometimes characterized as quasi-long-range order. Because of this property, such a state is usually called a crystal,[22] in spite of the fact that this state is not crystalline in the sense of classical crystallography.

The states we find, however, are never of this form, regardless of how weak the disorder (i.e., how large $d$) is. The reason is that isolated *dislocations* become included in the ground state configuration, which cannot be characterized by smooth displacements from a perfect crystal. (A dislocation is a site at which a line of electrons along a principal axis of the crystal comes to an end.) This type of defect spoils the quasi-long-range order associated with the "crystal" state.

Figure 2 illustrates several of the low-temperature states we have generated using our MD method, for different values of $d/a_0$. For large values of this parameter [Fig. 2(a)], isolated dislocations (denoted as bound pairs of + and × in the figures) may clearly be seen in the configuration. As $d$ is further increased, we have found that the density of dislocations decreases, until the average spacing between them exceeds our sample size. It is interesting to note that grain boundaries do not appear in our configurations. Some of the present literature on the WC has assumed that the effect of disorder is to introduce well-ordered microdomains, separated by sharp boundaries. This would be reflected in our configuration if the dislocations collected together to form grain boundaries.[23,24] We have found that this is not energetically favorable.

As the ratio $d/a_0$ is decreased [Figs. 2(b) and 2(c)], we

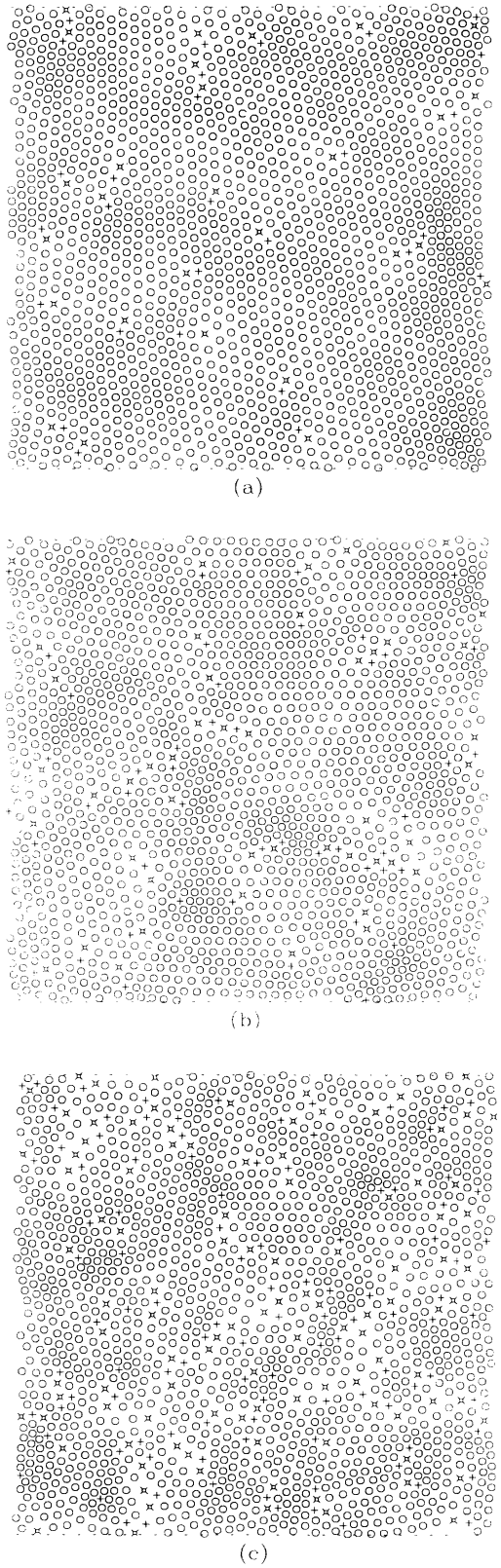

FIG. 2. Sample ground state configurations, for different levels of disorder. Locations of disclinations are marked by × for a sevenfold site, and + for a fivefold site. Bound pairs of these defects are equivalent to dislocations. Pictures contain $\approx$ 1600 particles; actual simulation samples contained 3200 particles. (a) $d/a_0 = 1.5$, (b) $d/a_0 = 1.2$, and (c) $d/a_0 = 1.0$.

have found that the ground state of the WC undergoes a zero-temperature phase transition, from a "hexatic glass" to an "isotropic glass." Both states must be characterized as glasses, because there is only short-range order in their positional correlation functions. The difference between these states may be understood in terms of defects called *disclinations*.[23,25] These are lattice points which have the incorrect number of nearest neighbors. In a perfect WC, which has a triangular lattice as its ground state,[7] disclination points may have (for example) five or seven nearest neighbors, whereas the perfect lattice points have six. A charge $s$ may be assigned to the disclinations, so that $s+6$ is the number of nearest neighbors surrounding the disclination. In the hexatic glass state, disclinations are present in tightly bound pairs ("neutral," in terms of disclination charge,) separated by a distance of order of a lattice constant. Such a bound pair is equivalent to a dislocation. One never finds isolated disclinations in this state. As the ratio $d/a_0$ is decreased, one may see disclination pairs which are separated by more than a single lattice constant, but are clearly still bound together. Below the critical setback distance, one can find isolated disclinations in the system.

As in the case of isolated dislocations, isolated disclinations tend to spoil correlations. The relevant correlation function for this disclination-unbinding transition measures the *orientational* order in the system. In the absence of isolated disclinations, the orientational correlation function falls off only as a power law (quasi-long-range order); when they are present, it falls off exponentially (short-range order). Figure 3 illustrates the orientational correlation functions for several values of $d/a_0$. (Precise definitions of the positional and orientational correlation functions will be given in Sec. III below.) We estimate from this that the transition between the states occurs near $d_c/a_0 = 1.15$. It must be noted that our simulations include neither the finite thickness of the layer, nor the finite value of the magnetic length $l_0$ when a magnetic field is present. Both these effects tend to soften the electron-electron interaction relative to the electron-ion interaction, so we expect the actual value of $d_c$ to be somewhat higher than this value. Nevertheless, it would be useful and interesting to look for this transition in real samples — either in heterostructures or on He film systems — as a function of $d/a_0$. A novel way of detecting the transition by measuring the depinning field is described below.

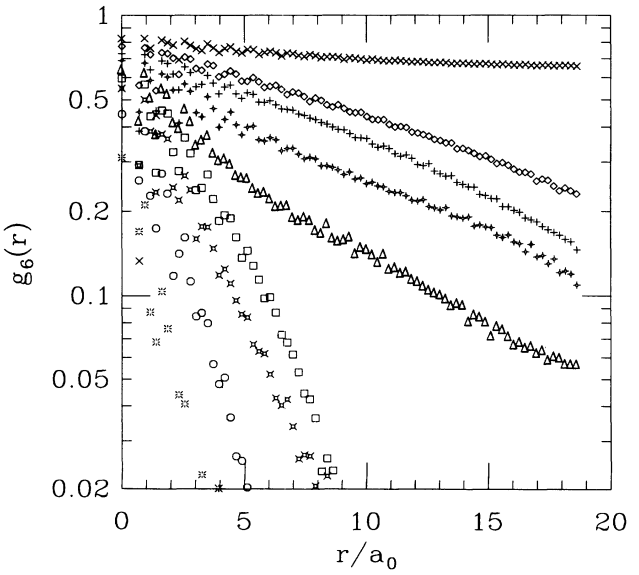


FIG. 3. Orientational correlation functions for various setback distances. Different symbols represent data for samples with different setback distances. From top to bottom, $d/a_0 = 2.0$, 1.7, 1.5 , 1.3 , 1.2 , 1.1, 1.0, 0.9, and 0.8.

Readers familiar with the Kosterlitz-Thouless-Halperin-Nelson-Young (KTHNY) theory of two-dimensional melting[25,22,26] will recognize the phenomenology of this transition. In the KTHNY theory, a two-dimensional crystal in the absence of quenched disorder but at finite temperatures undergoes two phase transitions as temperature is raised. At the lowest temperatures, thermally activated dislocations are bound together into pairs with equal and opposite Burger vectors.[27] This state is a crystal in the sense described above; there is a power-law decay in the positional correlation function. Furthermore, there is long-range order in the orientational correlation function. Above the Kosterlitz-Thouless melting temperature,[26] these pairs become unbound, and the crystal melts into a "hexatic" phase, characterized by short-range positional order and quasi-long-range orientational order. There are no isolated disclinations in this state. Finally, at a second higher temperature, the disclinations that make up the dislocations themselves unbind, and one finds both isolated dislocations and disclinations in typical configurations. Both the positional and the orientational correlation functions are short ranged, so that this state may be appropriately characterized as a liquid.

Clearly, the zero-temperature behavior of the electron solid in the presence of quenched disorder (i.e., the inherent disorder due to the random locations of the dopant ions) is partially analogous to this. In particular, we see an analog of the disclination-unbinding transition; however, the dislocations never pair together, even in the very weakly disordered case. It has been argued previously, based on a renormalization group analysis of a model closely related to ours, that a crystal is unstable with respect to the formation of free dislocations in the presence of arbitrarily weak quenched disorder.[28] Both these results — the absence of the crystal state, and the disclination-unbinding transition — may be understood from a continuum elasticity theory model of the electron crystal. The details of this analysis will be given elsewhere.[15]

It is interesting and instructive to see how the impurity driven disclination-unbinding transition is analogous to the temperature driven Kosterlitz-Thouless transition.[26] Here we present only the result; details will be presented elsewhere.[15] When one takes into account screening by dislocations,[29] it may be shown that the energy to create an isolated disclination (along with its screening cloud) has the form $E_1 = E_c \ln(A/a_0^2)$, where $A$ is the system area and $E_c$ is the core energy of a dislocation.

However, there is also an energy of interaction $E_2$ between the disclination and the free dislocations created by the impurities. If we consider an ensemble of disorder realizations, there will be a probability distribution $P(E_2)$ for $E_2$ to take on a particular value. The distribution of these energies we find[15,30] to take the form $\exp[-E_2^2/4\pi\rho_b a_0^2 E_c^2 \ln(A/a_0^2)]$, where $\rho_b$ is the dislocation density (in the absence of the disclination). The probability that it will be energetically favorable to create a disclination at a given site ($E_1 + E_2 < 0$) thus scales as $A^{-1/4\pi\rho_b a_0^2}$. Noting that the number of available sites to create a disclination scales as $A$, the total number of sites in a sample for which it is favorable to create a disclination scales as $A^{1-1/4\pi\rho_b a_0^2}$, and is nonvanishing in the infinite size limit if

$$\rho_b a_0^2 > \frac{1}{4\pi} \approx 1/14.$$

This is the analog of the original Kosterlitz-Thouless result.[26] We have found in our simulations that the transition appears to occur at slightly lower dislocation densities, around $\rho_b a_0^2 \approx 1/(20 \pm 2)$.

Beyond the ground state structure of the WC in the presence of quenched disorder, we have also investigated the depinning properties of this system. Figure 4 illustrates the trajectories of the electrons over a finite time interval for different values of $d/a_0$, for electric fields just above the depinning threshold. Figure 4(a) shows these trajectories for $d/a_0 = 1.5$. The motion of the electrons is quite uniform, and may be described as an elastic flow. It is important to note, however, that in the *time* domain, this flow is not as uniform as it appears in this figure: different patches of the WC actually move at different moments, so the motion is more of a "creep" than a flow. However, when averaged over a long enough time, the flow is uniform.

As the disorder increases [Fig. 4(b)], this creeping motion becomes more pronounced, with the waiting time for motion of certain patches sometimes becoming quite long. There is also an interesting and somewhat surprising phenomenon that becomes important as we pass from the hexatic to the isotropic glass: the direction of motion is correlated with the local crystal axis directions, so that the the local velocity is not exactly along the direction of the applied electric field. Because the system does not possess long-range orientational order, this means that different regions will slide in different directions, and in particular will at some locations "crash" into one another. For such grains, there may be long waiting times before the electrons at the regions where these merge can rearrange themselves and continue on. The rearrangement is often accompanied by the temporary formation of defects (dislocations or disclinations) which appear in the process of rearrangement. These regions clearly represent bottlenecks in the flow of the electrons, since crystal must become highly strained in order for the different flow directions to resolve themselves. Because of the rearrangement of the lattice in the process of sliding, this flow must be described as plastic. The importance of plastic flow in determining depinning properties has been emphasized recently for charge density wave (CDW) systems.[31]

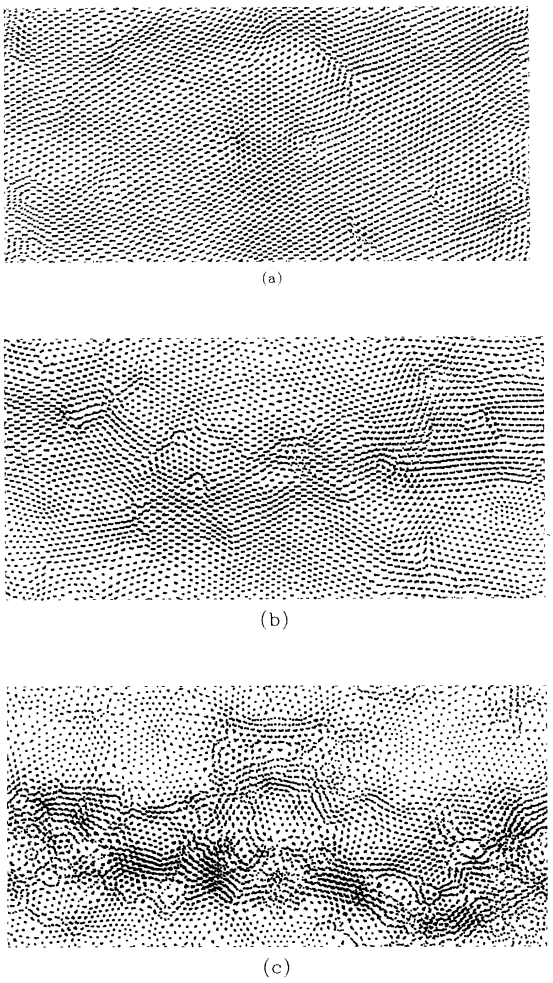


FIG. 4. Trajectory plots for 3200 particles for depinned WC with various levels of disorder. (a) $d/a_0 = 1.5$, (b) $d/a_0 = 1.2$, and (c) $d/a_0 = 0.9$, taken over a center of mass shift of $\Delta X/a_0 = 0.56, 0.44$, and 0.36, respectively.

At still stronger disorder strengths [Fig. 4(c)], the creep behavior completely dominates the motion of the electrons. In this limit, the wait time for some patches to move is longer than our simulation times; i.e., certain regions of the crystal never move at all. This means the solid "tears" when it depins. The flow in this limit appears channel-like, with only certain regions participating in carrying the current. Such channel-like motion has been observed previously in studies of the depinning properties of (and diffusive motion in) flux lattices in thin superconducting films.[32] Another important aspect of the motion that is not obvious from the trajectory plots is that the channels do not remain constant as a function of time: different channels appear to open and close as the simulations progress. Thus most of the particles do participate in the current, although at any given moment only a small percentage of them have a significant velocity.

Another interesting result of our work is the behavior of the threshold electric field $E_{th}$ for depinning as a

function of $d/a_0$. We find that the depinning field scales exponentially with the setback distance, as may be seen in Fig. 5. This effect may be understood if one assumes that the pinning is roughly determined by the strength of the electron-ion potential interacting with a perfect WC. This interaction scales approximately as[16,33] $e^{-Gd}$, where $G$ is a typical primitive reciprocal lattice vector magnitude, of order $2\pi/a_0$. It should be noted, however, that the defect structures induced by the disorder are also important in determining the strength of the depinning field. Configurations generated by relaxing an initially perfect crystal in the presence of the disorder potential, which does not allow isolated dislocations or disclinations to form in the resulting state, tend to have significantly smaller depinning fields than those containing these defects. The great sensitivity of $E_{th}$ to $d/a_0$ may potentially explain the rather large disparity found in measurements of the depinning field in different samples.[13]

A very unusual property of $E_{th}$ is its behavior in the vicinity of the transition from the hexatic to the isotropic glass. One can see a break in the curve in the vicinity of $d = 1.15a_0$, which we associate with the transition between states. Physically, we associate this break with the change in the orientational correlation functions in the vicinity of the transition. Since the flow patterns of the electrons as they depin follow the local orientational axes of the crystal, the bottlenecks in the flow occur where the electron motion must change directions, as described above. The number of such bottlenecks clearly will proliferate rapidly as the orientational order changes from exponential behavior to power-law behavior. This explains the increase in slope in Fig. 5 as $d/a_0$ drops below about 1.15. We note that the break is somewhat rounded, which we associate with the finite number of particles in our simulations. We have found that the break becomes slightly more rounded for smaller systems (although our error bars also increase for these simulations). We believe it is likely that this break will become sharper in the limit of infinite system sizes. An observation of such behavior in the depinning field would give direct evidence of a transition between the hexatic and isotropic glass ground states.

Finally, it is interesting to speculate what effect the creeping motion has on the noise spectrum in the current. In the simplest case of a sliding CDW, one expects the noise spectrum to have a narrow-band component, corresponding to the sliding of the (periodically arranged) electrons over the impurities.[11] The frequency of this noise component is proportional to the average velocity $v$ of the electrons.

Certainly for the case of our more disordered samples, this picture breaks down. The flow of electrons when they are depinned is plastic rather than elastic, so that the electrons do not preserve a local crystal symmetry particularly well as they are sliding. Furthermore, the opening and closing of various channels through the system introduces many time scales, contributing to a severe broadening of the noise spectrum.

Even at larger values of $d/a_0$, we do not observe a perfectly uniform motion of the electrons; we still observe a kind of creeping, jerky motion. Near the threshold voltage, the average time for the crystal to move one lattice constant, $a_0/v$, will become longer than the average time an individual electron remains stationary. In this circumstance one does not expect to observe narrow-band noise. Thus narrow-band noise should only be expected at voltages well above the threshold voltage for sliding. We have observed narrow-band noise in this circumstance in our simulations. Experimentally, however, it must be noted that finite currents can "heat" the electrons, which would lead to a melting of the crystal.[13,34] At present it is unclear whether the currents required for the narrow-band noise to become visible over the noise introduced by the creeping motion are low enough to avoid such effects in realistic samples. More detailed investigations of this issue are currently underway.

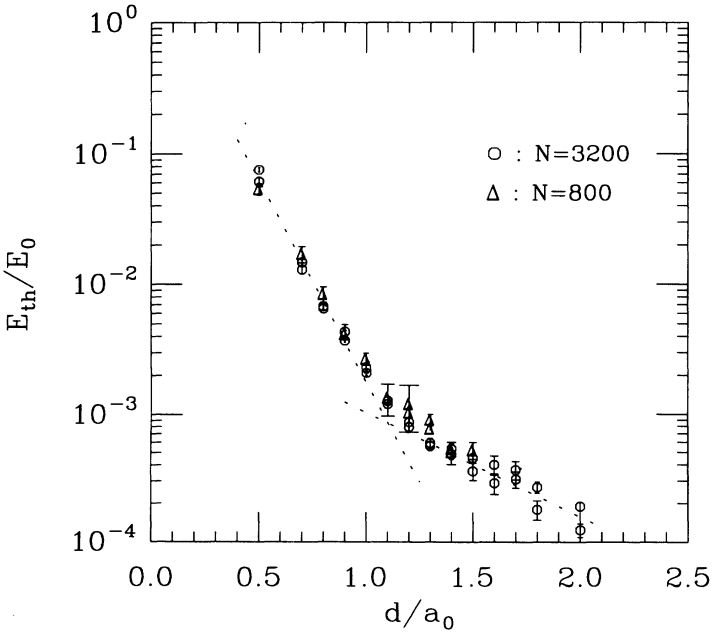


FIG. 5. Depinning threshold electric field, in units of $E_0 = e/\kappa a_0^2$. Dotted lines are guides to the eye.

## III. MOLECULAR-DYNAMICS AND SIMULATED-ANNEALING METHODS

Molecular dynamics is a powerful and well-known method for studying the motion of classical particles.[35] The central idea is the discretization of time, so that Newton's law $\vec{F}_i(t) = m\frac{d\vec{v}_i(t)}{dt}$ and the kinematic relation $\frac{d\vec{r}_i(t)}{dt} = \vec{v}_i$ may be rewritten as difference equations. Here, $\vec{F}_i(t)$, $\vec{v}_i(t)$, and $\vec{r}_i(t)$ are, respectively, the total force acting on particle $i$, the velocity of particle, and its position, at time $t$. The forces on a given particle in our simulations come from one of three sources: (1) interactions with other electrons,

$$\vec{F}_i^{ee} = \sum_{\vec{r}_j}{}' \frac{e^2}{\kappa|\vec{r}_i - \vec{r}_j|^3}(\vec{r}_i - \vec{r}_j),$$

where the prime in the sum indicates that $\vec{r}_i$ should not be included in the sum over $\vec{r}_j$, $e$ is the electronic charge, and $\kappa$ is the dielectric constant of the host medium; (2) interactions with the ions,

$$\vec{F}_i^{ei} = -\sum_{\vec{R}_j} \frac{e^2}{\kappa(|\vec{r}_i - \vec{R}_j|^2 + d^2)^{3/2}}(\vec{r}_i - \vec{R}_j),$$

where the $\vec{R}_j$'s are the ion positions in their setback plane; and (3) interactions with external forces (e.g., an external electric field.) We assume periodic boundary conditions, so that our system size is formally infinite, although it is periodic with a large but finite number of particles in each unit cell. The number $N$ of electrons (and ions) is taken to be 3200 in all the simulations reported here, except where specifically stated otherwise. Because of the long-range nature of the Coulomb interaction, the forces in (1) and (2) have to be computed using the Ewald sum technique,[7] which constitutes the bottleneck in our computations.

Part of our simulations require us to work at finite temperatures, which can be accomplished in one of two ways. In the microcanonical ensemble, we fix the total kinetic energy of the system to $Nk_BT$, where $k_B$ is Boltzmann's constant, and $T$ is the temperature. This is accomplished by rescaling the velocities by the rule $\vec{v}_i(t) \to \alpha\vec{v}_i(t)$, such that $\sum_i \frac{1}{2}mv_i^2 \equiv Nk_BT$ at every time step. The temperature of the system can be checked by examining the changes in the internal potential energy per particle of the system $U(t)/N$, where

$$U = \frac{1}{2}\sum_{i\neq j}\frac{e^2}{\kappa|\vec{r}_i - \vec{r}_j|} - \sum_{i,j}\frac{e^2}{\kappa(|\vec{r}_i - \vec{R}_j|^2 + d^2)^{1/2}} + \frac{1}{2}\sum_{i\neq j}\frac{e^2}{\kappa|\vec{R}_i - \vec{R}_j|}.$$

Note that the sums are over all the particles and ions in all the unit cells, and hence are a sum over an infinite number of particles. The last term in $U$ is independent of the electron positions and so does not contribute to its changes (the ion positions are quenched, and do not move in our simulations), but it is necessary to keep this term in order to get a finite result. When the system is in equilibrium, we find that at low temperatures $\overline{U_{T_1}(t)} - \overline{U_{T_2}(t)} = Nk_B(T_1 - T_2)$, where $U_T(t)$ is the configurational energy at temperature $T$ at time $t$ and the overbars represent time averages. Thus classical equipartition of the energy is satisfied when our simulations are in thermal equilibrium.

A second method for simulating the system at finite temperatures is to use the Langevin equation.[35,36] In this method, each electron $i$ is subjected to a white noise random force $\vec{\xi}_i(t)$ and a viscous force $F^\eta = -\eta\vec{v}_i$. The random force is connected to the temperature via the correlation function $\overline{\xi_i^\alpha(t)\xi_j^\beta(t')} = -2\eta k_BT\delta(t-t')\delta_{ij}\delta_{\alpha\beta}$, where $\alpha, \beta = x, y$. We have found that this method gives results similar to those obtained by the microcanonical ensemble. We will report in detail below our results as obtained in the latter method.

To obtain typical low energy configurations, we employ a simulated annealing method. Our procedure begins by assigning to the electrons random positions in the plane, and velocities according to a Gaussian distribution centered around our chosen temperature. The initial temperature is taken to be large enough that the electronic state is a liquid. The positions and velocities of the electrons are updated for several thousand time steps, in order to assure that the system is in thermal equilibrium. Once thermal equilibrium appears to have set in, the temperature is lowered by a small amount $\Delta T$, by rescaling all the velocities. This temporarily puts the system out of equilibrium, and it is necessary to update the system for several thousand time steps to equilibrate it. This process is repeated until the system approaches the melting temperature.

The melting transition in the absence of quenched disorder for two-dimensional classical electron systems has been studied via numerical methods by many authors.[22] The temperature of this system may be expressed in terms of the single unitless parameter $\Gamma = \sqrt{\pi\rho}e^2/\kappa k_BT$, which is the ratio of the average potential energy to the average kinetic energy of the system. In this expression, $\rho$ is the two-dimensional electron density. It is generally believed, based on Monte Carlo simulations,[37,22] that the electron crystal melts in the vicinity of $\Gamma = 130$. Thus the freezing temperature for our system should occur in the vicinity of 418 mK.

It is extremely important that in the annealing process the system spends a large number of time steps near and below this temperature in order to have a well-equilibrated system. The reason is that, once the system begins to freeze, defects will migrate very slowly. The energy barriers required to create or eliminate defects become quite high well below the freezing temperature, so that long annealing times are necessary to eliminate defects that should only be present at higher temperature. Thus it is necessary to equilibrate the system with a sufficient number of steps when temperature is below the melting point. We have checked this by slowing our annealing process (i.e., decreasing $\Delta T$ and increasing the number of time steps at each temperature) until the number of defects in the frozen state for a given impurity con-

figuration is essentially unchanged. Another nontrivial check that our annealing process equilibrates the system is to run it in the absence of any impurities (i.e., with a uniform neutralizing background), in which case the ground state should be defect-free. We have found that this is the case in most situations.[38]

The type of defects that are tracked in our simulations are the number of disclinations — i.e., the number of electrons with the incorrect number of nearest neighbors. As discussed in Sec. II, a dislocation is equivalent to a bound pair of disclinations, so implicitly this keeps track of the dislocations as well. The defects are located using the Voronoi polygon method,[39] which is a numerical method by which the Wigner-Seitz cell around each electron may be constructed; the number of nearest neighbors is then equal to the number of sides of the cell.

The results presented here are for very low temperatures compared to the melting temperature, typically of the order 20 mK. Finally, it should be noted that because of the finite annealing time, one cannot expect, if the temperature were lowered precisely to zero, that the resulting state found in our simulation would be the global ground state of the system. It clearly will be a low energy metastable state, and there is no reason to believe that it will be qualitatively different than the ground state. Thus for the properties we are interested in — correlation functions, number of defects, depinning fields — the annealed state should give qualitatively the same results as the true ground state of the system.

Some typical configurations are illustrated in Fig. 2, for various setback distances. As was mentioned in Sec. II, we have found that the system is always unstable against the formation of dislocations for any level of disorder (i.e., any value of $d/a_0$), and that isolated disclination starts to appear in the vicinity of $d/a_0 \leq 1.15$. The dislocations may be seen to appear in regions where there is a gradient in the electron density — i.e., there is a local change in the lattice constant of the WC. Physically, this may be understood in terms of the long-wavelength fluctuations in the positively charged ionic background. It is convenient to reexpress the ionic charge as a positively charged, nonuniform neutralizing background that is in the same plane as the electrons.[33] The long-wavelength behavior of WC will be essentially determined by charge neutrality: since maintaining charge imbalances over long distances is prohibitively expensive energetically, the WC will arrange itself in such a way as to neutralize this effective, spatially fluctuating positive charge.

This is essentially the driving force for the creation of dislocations. To see this, consider a region $\Omega$ of size scale $\xi$ with a slightly larger neutralizing background density than the average, $\rho_0 + \delta\rho$. The WC must raise its local density to neutralize this fluctuation. If this is done by smooth displacements from a perfect crystal, the resulting configuration will be strained in the vicinity of the region $\Omega$, with an energy cost scaling as $\xi^2$. The WC can lower its energy by introducing dislocations near the boundary of $\Omega$. These will allow lines of charge to be added or removed from $\Omega$, so that the crystal is essentially unstrained both inside and outside $\Omega$. The energy cost to introduce these dislocations[16,15] scales as $\xi \ln \xi$; thus for large enough $\xi$ — i.e., for long-wavelength fluctuations — it is energetically favorable to create highly separated dislocations. This is illustrated explicitly in Fig. 6. We have taken a small-sized system — 480 particles — and introduced a circular region $\Omega$ at the center of our unit cell with density $\rho_0 + \delta\rho, \delta\rho = \frac{6}{25}\rho_0$. In Fig. 6(a), we obtain a low-temperature configuration by a direct relaxation method,[24] which does not allow defects to be introduced in the final configuration. The strain in the lattice outside $\Omega$ is quite apparent. In Fig. 6(b), we have used our simulated-annealing method to find a low energy configuration. As may be seen, the strain has been relieved, at the expense of introducing several dislocations near the boundary. The configuration in Fig. 6(b) is lower in energy than that of 6(a), by approximately 90 mK.

In our model, the correlation function for such fluctuations in the effective in-plane neutralizing background

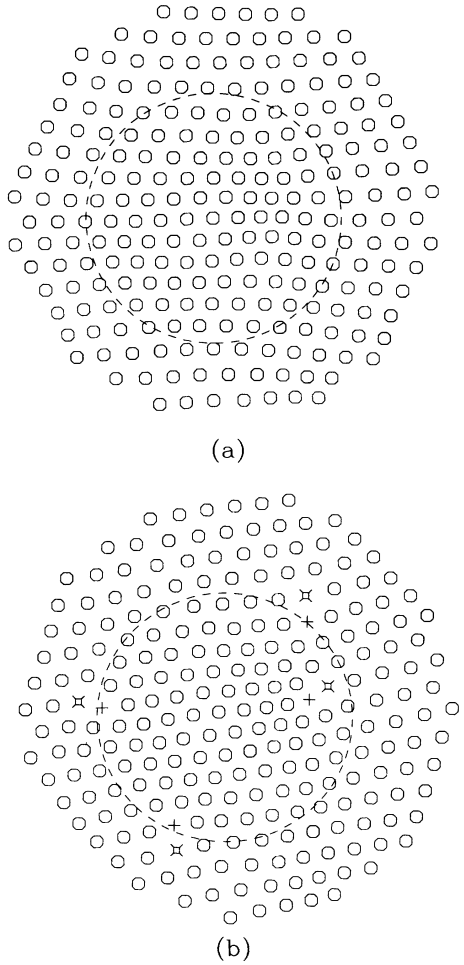


FIG. 6. At long wavelengths, the electron crystal density must track the disordered neutralizing background charge density. (a) Changing density with smooth displacements of an undefective WC produces a strained crystal in the region $\Omega$ circled by dotted lines. (b) Introducing dislocations in the region where the background density changes by $\delta\rho$ allows the electron density to match the background density without large regions of strain.

may be shown to be $\langle \rho_n(\vec{q})\rho_n(-\vec{q})\rangle = A\rho_0 e^{-2qd}$, where $\langle\,\rangle$ represents a disorder average, $\rho_n(\vec{q})$ is the Fourier transform of the effective in-plane neutralizing background charge density, $\rho_0 = N/A$ is the average density of ions, and $A$ is the system area. Note that as $d$ is increased, it is the *short*-wavelength fluctuations that are suppressed. However, since dislocations arise due to long-wavelength fluctuations in the disorder, we do not expect that large values of $d$ will suppress them. We have observed this behavior in our simulations.

As discussed in Sec. II, we have calculated both positional and orientational correlation functions for our low-temperature states. We conclude this section by giving precise definitions of these correlation functions.[40] The positional correlation function is given by

$$g(r) = \frac{\sum_{i,j}\delta(r - |\vec{r}_i - \vec{r}_j|)\frac{1}{6}\sum_{\vec{G}} e^{i(\vec{r}_i - \vec{r}_j)\cdot\vec{G}}}{\sum_{i,j}\delta(r - |\vec{r}_i - \vec{r}_j|)},$$

where $\vec{G}$ is a reciprocal lattice vector with the orientation which gives a peak of the structure factor. In practice, the $\delta$ function must be broadened so that it may be handled numerically. An example of the positional correlation function is illustrated in Fig. 7. The long distance tail of $g(r)$ falls off exponentially, indicating that there is only short-range positional order in the system. As stated in Sec. II, $g(r)$ has this behavior independent of whether it is in the hexatic or isotropic phase, i.e., for all values of $d$.

More interesting behavior is apparent in the orientational correlation function. In analogy with Ref. 25, this is defined as

$$g_6(r) = \frac{\sum_{i,j}\delta(r - |\vec{r}_i - \vec{r}_j|)\psi(\vec{r}_i)^*\psi(\vec{r}_j)}{\sum_{i,j}\delta(r - |\vec{r}_i - \vec{r}_j|)},$$

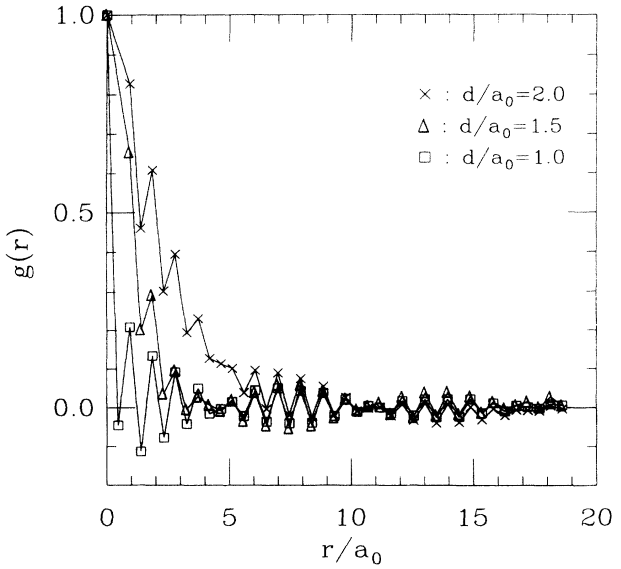


FIG. 7. Positional correlation functions for three different setbacks.

where $\psi(\vec{r}) = (1/n_c)\sum_{\alpha\in\{n.n.\}} e^{6i\theta_\alpha(\vec{r})}$ for an electron located at $\vec{r}$ with the bond angle $\theta_\alpha(\vec{r})$ with respect to the $x$ axis to the $\alpha$th nearest neighbor, summed over $n_c$ nearest neighbors determined by the Voronoi polygon method.[39]

Examples of $g_6$ are presented in Fig. 3, where the change in behavior in going from the isotropic to the hexatic phase is apparent. In particular, in the former case $g_6$ is short ranged, while in the latter we expect a power-law behavior at long distances.[25] Our simulations are consistent with this, although because of the finite size of our simulations it is difficult to distinguish between short-range order with a very long correlation length, and power-law behavior. However, direct estimates of the correlation length from $g_6$ in the interval $1.1 < d/a_0 < 1.2$ show that it increases very rapidly in the range, as would be expected for a critical phenomenon. We note that statistics for both $g$ and $g_6$ can in principle be improved by averaging over impurity configurations. Unfortunately, this is not practical, as the large size systems required ($\sim$ 3200 particles) to reliably

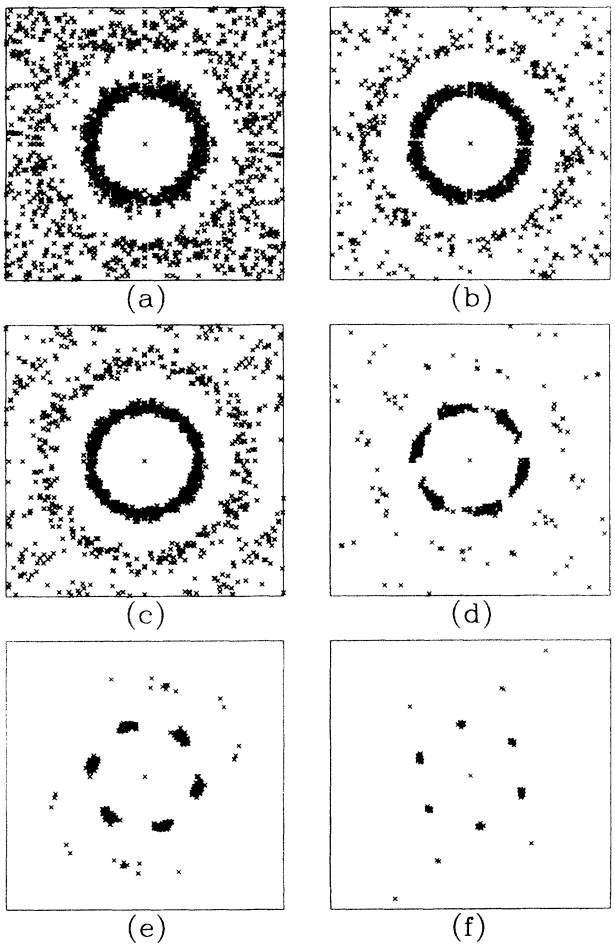


FIG. 8. Structure factor $S(\vec{q})$ in the reciprocal lattice vector space for samples with $d/a_0$ = (a) 0.8, (b) 1.0, (c) 1.1, (d) 1.2, (e) 1.4, (f) 1.7. Only points with $|S(\vec{q})| > \frac{1}{2}|S(\vec{q})|_{\max}$ are plotted. For large setback distances, a sixfold symmetry appears, indicating the presence of quasi-long-range orientational order.

measure the correlation functions in a single sample prohibit a large number of repetitions.

Another way of displaying the onset of hexatic order is to measure the structure factor. This is defined in the usual way as $|S(\vec{q})| = |\sum_i e^{i\vec{q}\cdot\vec{r}_i}|$, and is illustrated in Fig. 8 for several setback distances. For small setback distances $|S(\vec{q})|$ is essentially circularly symmetric; but as $d$ is increased, one can see six well-defined peaks developing for $d/a_0 \geq 1.2$. It should be noted that these are not Bragg peaks, in the sense that they do not become sharp in the large size limit; they instead remain as a modulation in an increasingly strong background.[25,40] Nevertheless, the presence of this modulation indicates the existence of some orientational order in the hexatic glass phase.

## IV. DEPINNING THRESHOLDS AND CURRENTS

In this section, we discuss the numerical method used to compute the threshold electric field above which the WC depins and the path the current follows above this threshold. Conceptually, the simplest way to do this is to begin with an annealed system, prepared as described in Sec. III, and then simulate a uniform electric field by subjecting all the particles to a constant force. In practice, however, this turns out to be computationally quite inefficient. The reason is that when the electric field is stepped up by an amount $\Delta E$, this represents a large, nonrandom "kick," after which the system must reequilibrate. These equilibration times turn out to be quite long, typically on the order of 5000 time steps for 3200 particles. If the electric field step $\Delta E$ is taken to be too large, or if the equilibration time is too short, one can reach a metastable state in which current flows for several thousand time steps, but then may abruptly stop when the random motion of the electrons around the moving center of mass equilibrates.

Figure 9 illustrates the current for such a sequence of electric field increments, in which the net electric field remains below the threshold. Occasionally, after a particular increment, one can see very large amplitude oscillations, far above that expected from simple random motion (e.g., first 2000 time steps in Fig. 9). Such large oscillations occur if the fluctuating center of mass happens to be moving in the same direction as the uniform force applied to the electrons at the moment it is incremented. Apparently this can set into motion very long-lived phonon modes, and one must wait long times for the energy in this mode to redistribute itself among the other phonon modes – i.e., for the phonon to decay. Such a process occurred at the moment the electric field was turned on in Fig. 9 (27 000th time step), and one can see that the resulting nonequlibrium oscillations did not settle down even after 4000 time steps.

A much more numerically efficient method for determining the depinning threshold using MD was developed by Brass and co-workers.[41] In this technique, one begins with an annealed low-temperature state, and then shifts all the particles by a small amount ($0.01a_0$ in our simulations). The MD method is then used to reequilibrate the system, *keeping the center of mass of the electrons fixed in position.* This last requirement is enforced by adding a small correction to the velocities of all the electrons at each update, $\Delta v(t)$, so that the center of mass velocity remains precisely zero at every time step. The pinning force, defined as the average force acting on an electron due only to the impurities, is then measured. The sequence is then repeated, until the total shift in position is of the order $1a_0 - 3a_0$.

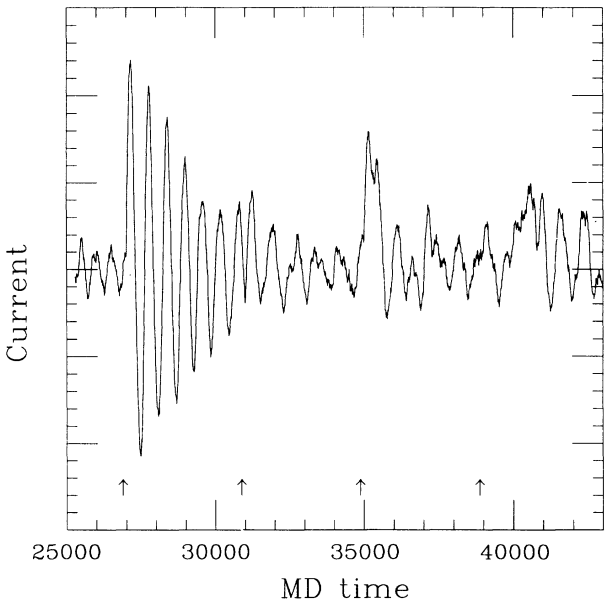


FIG. 9. Simulation of electric current for 3200 particles with electric field stepped up every 4000 time steps. The magnitude of fluctuations is clearly much greater than before the electric field is turned on, indicating the need for very long equilibration times between electric field steps.

The great numerical savings in this scheme is that the number of time steps required to equilibrate after a center of mass shift is quite small, only around 200 for 3200 particles. Thus the time required to find the threshold field in this manner is approximately an order of magnitude smaller than finding it by direct simulation of the electric field. Figure 10 illustrates the pinning force (represented as an electric field, by dividing out the electric charge) in a sequence of center of mass shifts. As can be seen, the pinning force rises monotonically (except for small fluctuations) to some maximum, and then abruptly drops. We associate this maximum with the depinning electric field. The trajectories of the particles for more disordered samples support this interpretation: one can see large rearrangements of the electrons ("channel-like flow") as the pinning force is decreasing. The sequence of steps gives several peaks of roughly the same order of magnitude, and the largest of these is chosen as the threshold electric field $E_{th}$. The variance among the peak heights gives a measure of the uncertainty in this quantity.

We note that we have compared $E_{th}$ for several samples, using both direct simulation of an electric field and

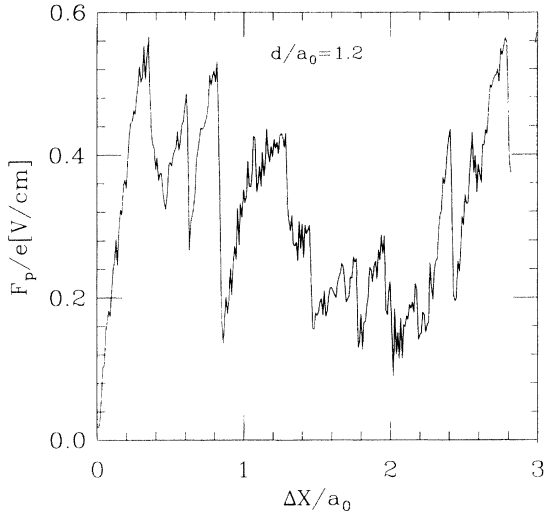


FIG. 10. Example of the pinning force vs center of mass shift $\Delta X$. Sharp peaks measure the depinning electric field, and give good agreeement with direct simulations of electric field depinning.

the shift method. The agreement between the thresholds found by these two methods is quite good. The qualitative behavior of the electronic motion for various levels of disorder found via the two methods – i.e., elastic flow vs plastic flow or channel-like flow – is also very similar.

Another detail that requires attention for the highly disordered samples is the fact that the disorder potential in general will favor certain regions for the channels through which the current may flow. Periodic boundary conditions can actually mask this effect, particularly if the channels are narrow, because in general a channel enters and exits at different points along the boundaries. This can lead to an overestimate of the pinning potential, since the final current channel may have to run through the sample many times before closing in on itself. Such narrow channel flow ("stringlike motion") has been observed in MD simulations of vortices in thin superconducting films, subject to a high degree of disorder.[32,41] To overcome this potential difficulty, we have used samples which have ion distributions that are mirror imaged across the $y$ axis through the center of the sample. Thus if the disorder potential favors relatively narrow channels, the crystal will not be pinned simply because the current has nowhere to go.

In practice, we have found that this consideration only affects our results for the most extremely disordered samples. Most of the electrons do eventually participate in the current, although they do not in general move at the same time. Even in the more disordered samples, where the flow is channel-like, the current channels are actually quite broad compared to what has been found in vortex systems.[32,41] Furthermore, different channels open and close with time, so that over the simulation time, current flows through most parts of the sample (although some patches do remain pinned throughout the simulation). Thus the disorder does not pick out a small region over which most of the current flows for the WC, except possibly at exceptionally small values of $d/a_0$.

Our results for the depinning field at various setback distances for a system of 3200 particles are shown in Fig. 5, and were discussed in Sec. II. As was noted, there is a noticeable break in $E_{th}$ vs $d$ in the range $d/a_0 = 1.1 - 1.2$, precisely where we see the transition between the hexatic and the isotropic glass phases. This may be understood in terms of the qualitative behavior of the electron motion as the disorder is turned up ($d$ decreased), changing the motion from elastic to plastic, channel-like flow. In the latter regime, especially near the hexatic-isotropic transition, there is a tendency for the flow to follow the local orientational axes of the crystal. Since the orientational correlation function changes from quasi long range to short range as $d$ is tuned through the transition, the number of changes in direction that a group of electrons will have to undergo in order to flow through the crystal increases rapidly once we enter the isotropic phase. The changes in direction represent bottlenecks in the motion, and cause the depinning field to increase rapidly as $d$ decreases. An experimental observation of this change of behavior in $E_{th}$ vs $d$ would represent a direct and unique way of probing the transition from the hexatic to the isotropic glasses. One might also note that the uncertainty in our results increases significantly with increasing $d$. This is because the number of defects in the system drops quickly in this limit, so that our results become more sensitive to finite size effects and fluctuations from one impurity realization to another. These uncertainties would certainly be reduced with studies of significantly larger systems, although this seems impractical at present from a numerical point of view.

Finally, we compare our results with recent calculations by Ruzin *et al.*[42] on pinning due to stray charged impurity ions that may lie relatively close to (i.e., a distance on the order of $a_0$ away from) the electron plane. This is relevant to modulation-doped semiconductor systems, in which a perfectly pure setback layer is in practice not possible to fabricate; small densities of donors and acceptors inevitably become incorporated in this layer. While detailed comparisons are difficult because little is known about the density and distribution of these unintentional dopants, we can speculate as to how they affect our results.

We note first that the state (i.e., hexatic or isotropic) of the system is unlikely to be affected by these impurities, since at such sparse densities they induce point defects (i.e., interstitials and vacancies) rather than extended defects, such as dislocations and disclinations. However, it is clear that for large enough setback distances $d$, the impurities in the volume of the setback layer will dominate the pinning properties. Using a density of $10^{13}$ $cm^{-3}$ positively charged donors,[43] and assuming that all these impurities lie at a distance from the electron plane that maximizes the pinning, we obtain an upper bound of $10^{-4}e/\kappa a_0^2$ for the pinning threshold due to these stray impurities. This is a very conservative estimate, and it should be noted that the true pinning threshold due to such impurities will likely be significantly lower than this.

[Indeed, in experimental systems with the largest setback ratios reported thus far[4,5] ($d/a_0 \approx 6$), the pinning threshold electric field is significantly smaller than this.] This estimate is near the bottom of our Fig. 5, so we do not expect it to affect our results for the hexatic-isotropic transition. Furthermore, an extrapolation of our results (Fig. 5) to large $d$ can give rough agreement with experimental samples.[44] Future samples with very large values of $d$ may well be dominated by stray impurities in their pinning properties. It is difficult to ascertain at this point – both because of the uncertainty in the density of these impurities, and the error bars in our calculations for large values of $d$ due to the finite size of our system – their relative importance in currently available semiconductor systems. Clearly, more work (both experimental and theoretical) is required to sort out this issue.

## V. SUMMARY

In this article, we have studied using molecular-dynamics techniques the low-temperature configurations and the depinning properties of the classical electron solid in the presence of disorder. Our calculations are applicable both to electrons on the surface of helium and to the two-dimensional electron gas in very strong magnetic fields. We have found evidence for a transition from a hexatic glass state to an isotropic glass state as a function of the disorder strength, which is characterized by the appearance of isolated disclinations, and the simultaneous loss of quasi-long-range orientational order as one passes from the former to the latter. This result indicates that the ground states of 2DEG's in modulation-doped semiconductors in the WC regime are *qualitatively* different in the weak and strong disorder regimes. We have found that the depinning threshold electric for the system increases rapidly (exponentially) with decreasing $d$, and that there is a break in $E_{th}$ vs $d$ in the vicinity of the transition between the states. An observation of the latter behavior in experiment would represent a direct probe of the transition. Finally, we observed a qualitative change in the motion of the electrons when they were depinned, from elastic flow in the very weakly pinned regime, to plastic, channel-like flow in the strongly pinned regime.

## ACKNOWLEDGMENTS

The authors thank Steve Girvin and Clayton Heller for helpful discussions. This work was supported by NSF Grant No. DMR92-02255. H.A.F. also acknowledges financial support from the A.P. Sloan Foundation and the Research Corporation.

[1] E.P. Wigner, Phys. Rev. **46**, 1002 (1934).
[2] C.C. Grimes and G. Adams, Phys. Rev. Lett. **42**, 795 (1979).
[3] R. Dingle, H.L. Störmer, A.C. Gossard, and W. Wiegmann, Appl. Phys. Lett. **33**, 655 (1978).
[4] V.J. Goldman, M. Santos, M. Shayegan, and J.E. Cunningham, Phys. Rev. Lett. **65**, 2189 (1990).
[5] H.W. Jiang, R.L. Willett, H.L. Störmer, D.C. Tsui, L.N. Pfeiffer, and K.W. West, Phys. Rev. Lett. **65**, 633 (1990).
[6] K. Maki and X. Zotos, Phys. Rev. B **28**, 4349 (1983).
[7] L. Bonsall and A.A. Maradudin, Phys. Rev. B **15**, 1959 (1977).
[8] There are also some indications that a WC can be stabilized without a magnetic field in related silicon metal-oxide-semiconductor field-effect transistor (MOSFET) systems. See V.M. Pudalov, M. D'Iorio, S.V. Kravchenko, and J.W. Campbell, Phys. Rev. Lett. **70**, 1866 (1993).
[9] R.L. Willett *et al.*, Phys. Rev. B **38**, 7881 (1988).
[10] H. Fukuyama and P.A. Lee, Phys. Rev. B **17**, 535 (1978); P.A. Lee and T.M. Rice, *ibid.* **19**, 3970 (1979).
[11] G. Gruner, Rev. Mod. Phys. **60**, 1129 (1988).
[12] F.I.B. Williams, P.A. Wright, R.G. Clark, E.Y. Andrei, G. Deville, D.C. Glattli, O. Probst, B. Etienne, C. Dorin, C.T. Foxon, and J.J. Harris, Phys. Rev. Lett. **66**, 3285 (1991).
[13] H.W. Jiang, H.L. Störmer, D.C. Tsui, L.N. Pfeiffer, and K.W. West, Phys. Rev. B **44**, 8107 (1991).
[14] Y.P. Li, T. Sajoto, L.W. Engel, D.C. Tsui, and M. Shayegan, Phys. Rev. Lett. **67**, 1630 (1991).
[15] H.A. Fertig and M.-C. Cha (unpublished).
[16] M.-C. Cha and H.A. Fertig, Phys. Rev. Lett. **73**, 870 (1994).
[17] H.W. Jiang and A.J. Dahm, Phys. Rev. Lett. **62**, 1396 (1989).
[18] C.A. Murray and D.H. Van Winkle, Phys. Rev. Lett. **58**, 1200 (1987).
[19] Y. Imry and S.K. Ma, Phys. Rev. Lett. **35**, 1399 (1975).
[20] N.D. Mermin, Phys. Rev. **176**, 250 (1968).
[21] A.B. Dzyubenko and Y.E. Lozovik, Surf. Sci. **263**, 680 (1992).
[22] For a review, see K. Strandburg, Rev. Mod. Phys. **60**, 161 (1988).
[23] F.R.N. Nabarro, *Theory of Crystal Dislocations* (Dover, New York, 1987).
[24] D.S. Fisher, B.I. Halperin, and R. Morf, Phys. Rev. B **20**, 4692 (1979).
[25] D.R. Nelson and B.I. Halperin, Phys. Rev. B **19**, 2457 (1979).
[26] J.M. Kosterlitz and D.J. Thouless, J. Phys. C **6**, 1181 (1973).
[27] The Burger vector of a dislocation measures the amount by which a circuit of steps between lattice sites around the core of a dislocation fails to close, if the steps in the circuit are chosen such that the path would close for a lattice without a defect. See Ref. 22.
[28] D.R. Nelson, Phys. Rev. B **27**, 2902 (1983).
[29] A previous study (Ref. 16) ignored dislocation screening effects, and found a crossover behavior rather than a phase transition, between states with few and many isolated disclinations. Screening effects of dislocations on the disclination change this to a true phase transition.
[30] The simplest assumption that generates this distribution is that the disorder generates a Gaussian white noise dis-

tribution of dislocations. A more realistic assumption, that seems to correspond quite well to our dislocation complexions in the weak disorder limit, is that a given lattice site may have a dislocation with probability $p$, or is a defect-free lattice site with probability $1-p$. The latter dislocation distribution gives results identical to the former.

[31] S.N. Coppersmith, Phys. Rev. Lett. **65**, 1044 (1990).

[32] A.C. Shi and A.J. Berlinsky, Phys. Rev. B **47**, 652 (1993); H.J. Jensen, A. Brass, A.C. Shi, and A.J. Berlinsky, *ibid.* **41**, 6394 (1990).

[33] H.A. Fertig and R. Côté, Phys. Rev. B **48**, 2391 (1993).

[34] In our simulations, we fix the temperature of the electrons at some value, which is equivalent to assuming perfect contact between the electron gas and a thermal reservoir. Electron heating thus does not occur in our simulations.

[35] R.W. Hockney and J.W. Eastwood, *Computer Simulation Using Particles* (IOP, Philadelphia, 1992); M.P. Allen and D.J. Tildesley, *Computer Simulation of Liquids* (Oxford University Press, New York, 1987).

[36] R. Balescu, *Equilibrium and Nonequilibrium Statistical Mechanics* (Wiley, New York, 1975).

[37] R.C. Gann, S. Chakravarty, and G.V. Chester, Phys. Rev. B **20**, 326 (1979).

[38] Occasionally, electrons in the absence of quenched disorder may freeze into a crystal with an orientation that does not match our boundary conditions. In this situation, a small number of defects will be incorporated in the ground state. The number of such defects is always much smaller than the number that we find in the presence of impurities, and we believe that such possible global misorientations are not relevant for the levels of disorder we have investigated.

[39] M.P. Allen, D. Frenkel, and W. Gignac, J. Chem. Phys. **78**, 4206 (1983).

[40] D. R. Nelson, M. Rubinstein, and F. Spaepen, Philos. Mag. A **46**, 105 (1982).

[41] A. Brass, H.J. Jensen, and A.J. Berlinsky, Phys. Rev. B **39**, 102 (1989); H.J. Jensen, A. Brass, and A.J. Berlinsky, Phys. Rev. Lett. **60**, 1676 (1988).

[42] I.M. Ruzin, S. Marianer, and B.I. Shklovskii, Phys. Rev. B **46**, 3999 (1992).

[43] Ruzin *et al.* (Ref. 42) conclude that acceptors are not as effective at pinning as donors in macroscopically sized samples.

[44] Since our error bars are relatively large for larger values of $d$, and the scale in Fig. 5 is logarithmic, such an extrapolation is subject to very large uncertainties.